

X-ray Absorption Factors for Ellipsoidal Crystals*

BY D. R. FITZWATER

Institute for Atomic Research and Department of Chemistry, Iowa State University, Ames, Iowa, U.S.A.

(Received 27 January 1960 and in revised form 17 June 1960)

The absorption factor integral for a general ellipsoidal crystal was transformed to spherical polar coordinates. The resulting exponential in the integral was expanded in a power series and the triple integration was carried out term by term. The process was stopped after the fifth order term but could be carried further. Four integrals could not be directly integrated and were evaluated by series expansions and integrations. The resulting series were tabulated as a function of one parameter. The termination of the absorption factor series with the fifth order term gives results for a sphere with < 2% error for $\mu R = 1.0$.

Introduction

The ellipsoidal crystal is a good approximation to many real crystal forms, and ellipsoidal absorption factor corrections should be satisfactory for film accuracies with many crystal forms. In addition, grinding an anisotropic crystal quickly produces ellipsoids and may not produce spheres even after continued grinding. The size of the final spheres, if any, may also be too small. Consequently, very accurate ellipsoidal corrections are useful for counter work with such crystals.

The difficulty of carrying out the required integration in such a case for each reflection is prohibitive. Because of the large number of parameters affecting the ellipsoidal absorption factor, tabulation of the absorption factor is not feasible. The only remaining possibility is to obtain the ellipsoidal absorption factor as a function of its parameters. This required an analytical integration of the expression

$$A = 1/V_c \int_{\substack{\text{crystal} \\ \text{volume}}} \exp \{-\mu(\rho_1 + \rho_2)\} dV, \quad (1)$$

where A is the absorption factor, V_c is the volume of the crystal, μ is the linear absorption coefficient for the crystal, ρ_1 and ρ_2 are the path lengths in the crystal of the incoming and diffracted X-ray beam element. By expanding the exponential in the integrand, the integration may be carried out. The labor of integrating each term of the series is such that the series is terminated as soon as is possible. The choice made here gives, in the special case of a sphere, accurate absorption factors up to a μR of 1.4. This is a very useful range for crystals with $\mu \lesssim 100$.

Derivation of the absorption factor equation

The first step is to express (1) in a more suitable coordinate system. The transformation

$$x'_i = x_i/a_i \quad (i = 1, 2, 3) \quad (2)$$

has the Jacobian $a_1 a_2 a_3$, where the a_i are the axes of the ellipsoid. The absorption factor (1) can now be written as

$$A = (1/V_c) \int \exp \{-\mu(\rho_1 + \rho_2)\} a_1 a_2 a_3 dV', \quad (3)$$

where $dV' = dx'_1 dx'_2 dx'_3$. Since the volume of the crystal is

$$V_c = \frac{4}{3} \pi a_1 a_2 a_3 \quad (4)$$

the $a_1 a_2 a_3$ factor in (3) will cancel. The limits of integration in (1) correspond to the surface of the ellipsoid

$$\sum_{i=1}^3 (x_i/a_i)^2 = 1, \quad (5)$$

where x_i are the components of a vector from the origin to the surface of the ellipsoid. The transformation (2) now gives as the limiting surface

$$\sum_{i=1}^3 (x'_i)^2 = 1, \quad (6)$$

which is a sphere of unit radius. We can now write (1) as

$$A = \frac{3}{4\pi} \int_{\substack{\text{unit} \\ \text{sphere}}} \exp \{-\mu(\rho_1 + \rho_2)\} dV'. \quad (7)$$

The index $i = 1, 2$ will be used to denote the variables referring to the incoming and outgoing X-ray beam. Thus ρ_i represents either ρ_1 or ρ_2 . Let \mathbf{n}_1 represent a unit vector defining the direction of the incoming X-ray beam and let \mathbf{n}_2 represent a unit vector defining the negative of the outgoing X-ray beam direction. Let \mathbf{r}_i represent a vector from the origin to the entrance point on the ellipsoidal surface of \mathbf{n}_i . Let \mathbf{r} represent a vector from the origin to the volume element under consideration. The relationships of these vectors are shown in Fig. 1.

* Contribution No. 803. Work was performed in the Ames Laboratory of the U.S. Atomic Energy Commission.

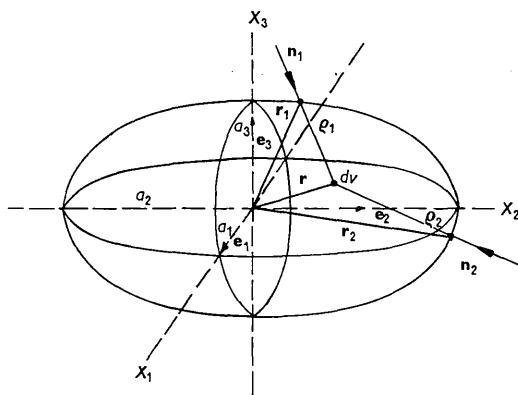


Fig. 1. Coordinate system for the ellipsoid, based on unit vectors \mathbf{e}_i along the axes of the ellipsoid. \mathbf{n}_1 is a unit vector in direction of incoming X-ray beam and \mathbf{n}_2 is a unit vector in the direction opposite to the outgoing X-ray beam. q_i are corresponding path lengths in the crystal.

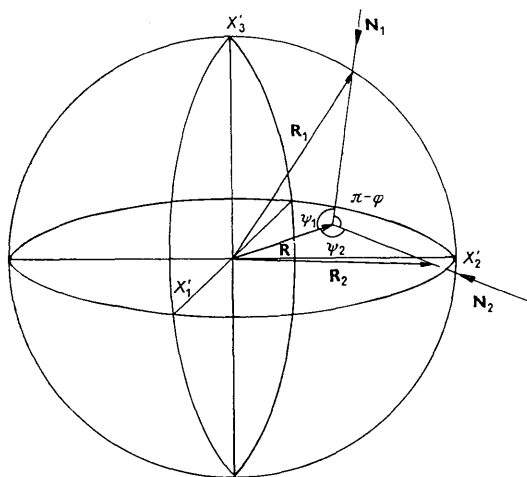


Fig. 2. Transformed coordinate systems. Each vector component is obtained from the vectors of Fig. 1 by dividing by the corresponding ellipsoidal axis. The equation for the ellipsoid goes into an equation for a sphere under this transformation.

By transforming the vectors in Fig. 1 as in (2), we obtain the corresponding capital letter vectors of Fig. 2, where \mathbf{N}_i are no longer unit vectors. We must now obtain an expression for q_i . We have, from Fig. 1,

$$\mathbf{r}_i = \mathbf{r} - q_i \mathbf{n}_i, \quad (8)$$

which becomes

$$\mathbf{R}_i = \mathbf{R} - q_i \mathbf{N}_i \quad (9)$$

after transformation by (2). Since

$$R_i = 1, \quad (10)$$

we can solve (10) for q_i and obtain

$$q_i = 1/N_i \{ R \cos \psi_i + [1 - R^2 \sin^2 \psi_i]^{1/2} \}, \quad (11)$$

where

$$\mathbf{R} \cdot \mathbf{N}_i = R N_i \cos \psi_i. \quad (12)$$

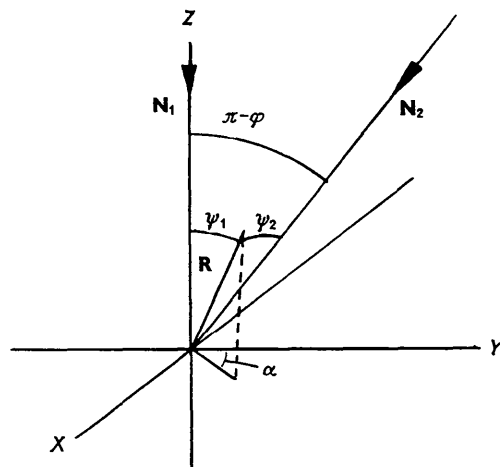


Fig. 3. Spherical polar coordinates. The coordinate axes X , Y and Z are chosen as above for convenience in the derivation of (13). (\mathbf{N}_1 is parallel to Z and \mathbf{N}_2 is in the YZ plane.)

If (7) is transformed into spherical polar coordinates as in Fig. 3, the integration can be carried out after expressing ψ_2 in terms of ψ_1 as

$$\cos \psi_2 = \cos \psi_1 \cos (\pi - \varphi) + \sin \psi_1 \sin (\pi - \varphi) \cos \alpha. \quad (13)$$

Interchange of N_1 and N_2 will not affect the value of the integral, and so interchanging subscripts in (13) simply amounts to a change in the definition of the polar coordinates. Consequently, as a result of this invariance, we can write

$$\int (N_1 q_1)^n (N_2 q_2)^m dV' = \int (N_1 q_1)^m (N_2 q_2)^n dV'. \quad (14)$$

Expansion of the integrand of (7) in a power series gives

$$\begin{aligned} \exp -\mu (q_1 + q_2) &= \sum_j \frac{(-\mu)^j (q_1 + q_2)^j}{j!} \\ &= \sum_j \sum_p \frac{1}{(j)!} \binom{j}{p} \frac{(-\mu)^j}{N_1^p N_2^{j-p}} (N_1 q_1)^p (N_2 q_2)^{j-p}. \end{aligned} \quad (15)$$

If we now integrate this expression, while using (14) to combine terms, we obtain

$$\begin{aligned} A &= \frac{3}{4\pi} \left[1 - \mu \left(\frac{1}{N_1} + \frac{1}{N_2} \right) \int f_1 dV' + \frac{\mu^2}{2!} \left(\frac{1}{N_1^2} + \frac{1}{N_2^2} \right) \int f_1^2 dV' \right. \\ &\quad + \frac{\mu^2}{2!} \left(\frac{2}{N_1 N_2} \right) \int f_1 f_2 dV' - \frac{\mu^3}{3!} \left(\frac{1}{N_1^3} + \frac{1}{N_2^3} \right) \int f_1^3 dV' \\ &\quad \left. - \frac{3\mu^3}{3!} \left(\frac{1}{N_1^2 N_2} + \frac{1}{N_1 N_2^2} \right) \int f_1^2 f_2 dV' + \dots \right], \end{aligned} \quad (16)$$

where $f_i = N_i q_i$. The majority of the integrals required in (16) can be expressed in terms of other, simpler, integrals and either evaluated directly or by the use of the definite integrals compiled by DeHaan (1939).

Even so, the process is quite tedious. There is no reason, other than the labor involved, why the process could not be continued through additional terms. At the present time the integration is carried out through the terms involving μ^5 . The addition of only a few extra terms would increase substantially the range of convergence of the resulting series because the factorial in the denominator is just becoming dominant. At this point, there remain only four integrals involving, among other quantities, products of $[1 - R^2 \sin^2 \psi_1]^{\frac{1}{2}} [1 - R^2 \sin^2 \psi_2]^{\frac{1}{2}}$ which could not be evaluated. In each such case, the argument was expanded in multiple power series and the general term integrated. The resulting series were then summed by writing a For Transit program for the IBM 650. These integrals are only a function of φ and do not vary rapidly. Consequently, it was sufficient to carry out the summations for only a relatively few values of φ and to use Lagrangian interpolation to sub-tabulate.

The series expression for A was terminated at the point where the factorial in the denominator is becoming dominant. Consequently, convergence above $\mu R=1$ for the limiting case of a sphere is very poor. Since the series is an alternating series, the use of the Euler transformation as described by Booth (1955) leads to great improvement in accuracy near the values of $\mu R=1$ and extends the useful accuracy to $\mu R=1.4$. The Euler transformation gives the sum of the series

$$S = \sum_{i=0}^{\infty} (-1)^i u_i \quad (17)$$

as

$$S = \frac{1}{2} [u_0 - \frac{1}{2} \Delta u_0 + \frac{1}{4} \Delta^2 u_0 - \frac{1}{8} \Delta^3 u_0 + \dots], \quad (18)$$

where $\Delta u_0 = u_1 - u_0$. The best results are obtained by summing the first three terms directly and transforming the last three.

Checking procedures

The series for A evaluated at $\varphi=0, \pi$ for a sphere was checked term by term with the results of the exact integration. The final results for a sphere were in good agreement at $\varphi=0, \pi/4, \pi/2, 3\pi/4, \pi$ with the corresponding values obtained by Bond (1959) for a sphere.

The integrals which were evaluated by summation were checked term by term against the exact integration at $\varphi=0, \pi$. The For Transit program was subjected to careful checking and hand calculation of random terms for comparison.

Absorption factor equation

After the evaluation of the numerous integrals in (16), we can write

$$\begin{aligned} A = & 1 - \mu \left(\frac{1}{N_1} + \frac{1}{N_2} \right) \frac{3}{4} + \mu^2 \left(\frac{1}{N_1^2} + \frac{1}{N_2^2} \right) \frac{2}{5} \\ & + \mu^2 \frac{1}{N_1 N_2} \left[K_1(\varphi) - \frac{1}{5} \cos \varphi \right] - \mu^3 \left(\frac{1}{N_1^3} + \frac{1}{N_2^3} \right) \frac{1}{6} \\ & - \mu^3 \left(\frac{1}{N_1^2 N_2} + \frac{1}{N_1 N_2^2} \right) \left[\frac{7}{24} - \frac{1}{6} \cos \varphi + \frac{1}{24} \cos^2 \varphi \right] \\ & + \mu^4 \left(\frac{1}{N_1^4} + \frac{1}{N_2^4} \right) \frac{2}{35} + \mu^4 \left(\frac{1}{N_1^3 N_2} + \frac{1}{N_1 N_2^3} \right) \\ & \quad \times \left[K_2(\varphi) - \frac{3}{35} \cos \varphi \right] \\ & + \mu^4 \left(\frac{1}{N_1^2 N_2^2} \right) \left[\frac{1}{7} + \frac{2}{35} \cos^2 \varphi - K_3(\varphi) \cos \varphi + K_4(\varphi) \right] \\ & - \mu^5 \left[\frac{1}{N_1^5} + \frac{1}{N_2^5} \right] \frac{2}{5!} - \mu^5 \left(\frac{1}{N_1^4 N_2} + \frac{1}{N_1 N_2^4} \right) \frac{1}{5!} \left[\frac{109}{24} \right. \\ & \quad \left. - 4 \cos \varphi + \frac{9}{12} \cos^2 \varphi - \frac{1}{8} \cos^4 \varphi \right] \\ & \quad - \mu^5 \left[\frac{1}{N_1^3 N_2^2} + \frac{1}{N_1^2 N_2^3} \right] \left[\frac{13}{2} \right. \\ & \quad \left. - \frac{14}{3} \cos \varphi + \frac{9}{2} \cos^2 \varphi - \frac{13}{3} \cos^3 \varphi \right] + \dots \quad (19) \end{aligned}$$

Each $K_i(\varphi)$ is not a single integral but a combination of the four integrals mentioned above. For $i=1, 2, 3$, $K_i(\varphi) = K_i(\pi - \varphi)$ and for $i=4$, $K_4(\varphi) = -K_4(\pi - \varphi)$. The values of $K_i(\varphi)$ are given in Table 1, and selected values of A for the limiting case of a sphere are given in Tables 2, 3, and 4. Linear interpolation can be used in Table 1. The values $A(\varphi)$ in Tables 2, 3, and 4 are taken from Bond (1959). The values $A'(\varphi)$ are the direct summation of (19). The values of $A''(\varphi)$ are those of the sum of the series after the Euler transformation.

Table 1. Values of $K_i(\varphi)$

| φ° | K_1 | K_2 | K_3 | K_4 |
|-----------------|--------|--------|--------|--------|
| 0 | 0.6000 | 0.1429 | 0.1427 | 0.0000 |
| 9 | 0.5990 | 0.1420 | 0.1419 | 0.0015 |
| 18 | 0.5966 | 0.1405 | 0.1395 | 0.0044 |
| 27 | 0.5924 | 0.1377 | 0.1355 | 0.0088 |
| 36 | 0.5881 | 0.1342 | 0.1304 | 0.0133 |
| 45 | 0.5828 | 0.1303 | 0.1246 | 0.0163 |
| 54 | 0.5772 | 0.1261 | 0.1188 | 0.0171 |
| 63 | 0.5721 | 0.1224 | 0.1134 | 0.0153 |
| 72 | 0.5682 | 0.1193 | 0.1090 | 0.0115 |
| 81 | 0.5658 | 0.1174 | 0.1061 | 0.0061 |
| 90 | 0.5650 | 0.1167 | 0.1051 | 0.0000 |

The values in Tables 2, 3, and 4 give a measure of the accuracy of the series. In the general case, the accuracy can vary more from reflection to reflection than in the spherical case, due to the varying values of the N_i . A good measure of the accuracy in an individual case is the value of the last term in the transformed series.

Table 2. Selected values of $A(0)$ for a sphere

| μR | A | A' | A'' |
|---------|--------|---------|--------|
| 0.1 | 0.8621 | 0.8613 | — |
| 0.4 | 0.5555 | 0.5556 | — |
| 0.8 | 0.3175 | 0.3109 | 0.3238 |
| 0.9 | 0.2770 | 0.2644 | 0.2831 |
| 1.0 | 0.2427 | 0.2191 | 0.2470 |
| 1.1 | 0.2128 | 0.1719 | 0.2146 |
| 1.2 | 0.1869 | 0.1196 | 0.1851 |
| 1.3 | 0.1645 | 0.0581 | 0.1580 |
| 1.4 | 0.1449 | -0.0175 | 0.1329 |
| 1.5 | 0.1282 | -0.1129 | 0.1096 |

Table 3. Selected values of $A(\pi/2)$ for a sphere

| μR | A | A' | A'' |
|---------|--------|---------|--------|
| 0.1 | 0.8621 | 0.8628 | — |
| 0.4 | 0.5714 | 0.5727 | — |
| 0.8 | 0.3534 | 0.3340 | 0.3545 |
| 1.0 | 0.2857 | 0.2215 | 0.2810 |
| 1.2 | 0.2353 | 0.1030 | 0.2206 |
| 1.4 | 0.1969 | -0.2247 | 0.1705 |
| 1.5 | 0.1812 | -0.4399 | 0.1495 |

Table 4. Selected values of $A(\pi)$ for a sphere

| μR | A | A' | A'' |
|---------|--------|---------|--------|
| 0.1 | 0.8621 | 0.8648 | — |
| 0.4 | 0.5882 | 0.5886 | — |
| 0.8 | 0.3922 | 0.3411 | 0.3921 |
| 1.0 | 0.3322 | 0.1476 | 0.3238 |
| 1.2 | 0.2865 | -0.2312 | 0.2700 |
| 1.4 | 0.2513 | -0.9787 | 0.2323 |

Since $1/N_i \leq R$, where R is the radius of a sphere containing the ellipsoid, the possible error for the ellipsoid is less than that for the worst diffraction angle of the surrounding sphere. However, this error relationship has not been demonstrated for the transformed series.

Method of application

The absorption factor (19) is expressed in terms of μ , N_i , and φ . The value of μ can be obtained from the composition and density of the crystal. φ is defined by

$$\mathbf{N}_1 \cdot \mathbf{N}_2 = -N_1 N_2 \cos \varphi, \quad (20)$$

where

$$\mathbf{N}_i = \begin{pmatrix} 1/a_1 & 0 & 0 \\ 0 & 1/a_2 & 0 \\ 0 & 0 & 1/a_3 \end{pmatrix} \mathbf{n}_i. \quad (21)$$

The values of a_i are obtained by direct measurement of the crystal. All that remains to be supplied are the \mathbf{n}_i .

The values of \mathbf{n}_i depend upon the diffraction technique, the orientation of the reciprocal lattice and the orientation of the ellipsoid. Let \mathbf{h} be a reciprocal lattice vector and define \mathbf{x} as

$$\mathbf{x} = T\mathbf{h}, \quad (22)$$

where \mathbf{x} is \mathbf{h} expressed in a suitable set of crystal cartesian coordinates, described by the unit vectors \mathbf{e}_i .

Diffraction occurs when some machine operation R brings \mathbf{x} into alignment with the diffraction vector \mathbf{d} ,

$$R\mathbf{x} = \mathbf{d} = \mathbf{s} - \mathbf{s}_0, \quad (23)$$

where \mathbf{s} is the direction of the diffracted beam and \mathbf{s}_0 is the direction of the incident beam. \mathbf{s} , \mathbf{s}_0 and \mathbf{x} are expressed in the same crystal cartesian coordinate system. We can now write

$$\begin{aligned} \mathbf{n}'_1 &= R^{-1}\mathbf{s}_0, \\ \mathbf{n}' &= -R^{-1}\mathbf{s}. \end{aligned} \quad (24)$$

If S transforms a vector in crystal cartesian coordinates to a vector in the cartesian coordinates of the ellipsoid as in Fig. 1, we now have

$$\mathbf{n}_i = S(\mathbf{n}'_i/n_i). \quad (25)$$

All of the quantities in (19) are now available. As an example, the specific equations for \mathbf{n}_i will be derived for several diffraction methods.

Single crystal orienter

Choose the crystal cartesian coordinate system with unit vector \mathbf{e}_2 in the direction of the X-ray source when $2\theta=0$ and unit vector \mathbf{e}_3 along the axis of the goniometer head with $\chi=0$.

The operating design of the General Electric single crystal orienter requires

$$\begin{aligned} \mathbf{d} &= d\mathbf{e}'_1, \\ R &= R_1(\chi)R_2(\varphi)R_1^{-1}(\chi)R_1(\chi), \end{aligned} \quad (26)$$

or

$$R = R_1(\chi)R_2(\varphi),$$

where $R_1(\chi)R_2(\varphi)R_1^{-1}(\chi)$ represents the φ motion and $R_1(\chi)$ represents the χ motion of the single crystal orienter. The angle φ as used in this section is not the same as the previous angle φ . φ is used in this section because of the single crystal orienter terminology. The explicit forms of R_2 and R_1 , are given by

$$R_2(\varphi) = \begin{pmatrix} \cos \varphi & \sin \varphi & 0 \\ -\sin \varphi & \cos \varphi & 0 \\ 0 & 0 & 1 \end{pmatrix},$$

and

$$R_1(\chi) = \begin{pmatrix} \cos \chi & 0 & \sin \chi \\ 0 & 1 & 0 \\ -\sin \chi & 0 & \cos \chi \end{pmatrix}. \quad (27)$$

We can now write,

$$\begin{aligned} \mathbf{s}_0 &= R_2^{-1} \left(\frac{3\pi}{2} - \theta \right) \mathbf{d}, \\ \mathbf{s} &= R_2^{-1} \left(\frac{3\pi}{2} + \theta \right) \mathbf{d}. \end{aligned} \quad (28)$$

Substitution of (28) into (24) and using (26) leads to

$$\begin{aligned} \mathbf{n}'_1 &= R_2^{-1}(\varphi) R_1^{-1}(\chi) R_2^{-1}\left(\frac{3\pi}{2} - \theta\right) \mathbf{d} \\ \mathbf{n}'_2 &= -R_2^{-1}(\varphi) R_1^{-1}(\chi) R_2^{-1}\left(\frac{3\pi}{2} + \theta\right) \mathbf{d} \end{aligned} \quad (29)$$

and then

$$\begin{aligned} \mathbf{n}'_1 &= xR_2(-\varphi)R_1(-\chi) \begin{pmatrix} -\sin \theta \\ -\cos \theta \\ 0 \end{pmatrix} \\ \mathbf{n}'_2 &= xR_2(-\varphi)R_1(-\chi) \begin{pmatrix} \sin \theta \\ -\cos \theta \\ 0 \end{pmatrix}. \end{aligned} \quad (30)$$

The angles θ , φ , χ are obtained as the solution of the equation

$$R_2(-\varphi)R_1(-\chi)\mathbf{d} = \mathbf{x} \quad (31)$$

and are given by

$$\begin{aligned} \theta &= \sin^{-1} \lambda x/2, \\ \varphi &= \tan^{-1} x_2/x_1, \\ \chi &= \sin^{-1} x_3/x. \end{aligned} \quad (32)$$

Substitution of (30) into (25) now gives the required \mathbf{n}_i values.

Equi-inclination Weissenberg

Define the crystal cartesian coordinate system, so that \mathbf{s}_0 lies in the plane containing \mathbf{e}'_2 and \mathbf{e}'_3 for any value of μ , and \mathbf{s} lies in a cone whose axis is \mathbf{e}'_3 . The crystal is to be rotated about \mathbf{e}'_3 to the diffracting position.

We can now write

$$\begin{aligned} \mathbf{s}_0 &= \frac{1}{\lambda} \begin{pmatrix} 0 \\ \cos \mu \\ -\sin \mu \end{pmatrix} \\ \mathbf{s} &= \frac{1}{\lambda(1 + \sin^2 \mu)^{\frac{1}{2}}} \begin{pmatrix} \sin \psi \\ \cos \psi \\ \sin \mu \end{pmatrix} \end{aligned} \quad (33)$$

where λ is the wavelength of radiation used, and ψ is the angle between \mathbf{e}'_2 and the projection of \mathbf{s} onto the plane containing \mathbf{e}'_1 and \mathbf{e}'_2 . We can now solve the equation for the Bragg angle 2θ ,

$$\mathbf{s} \cdot \mathbf{s}_0 = \frac{1}{\lambda^2} \cos 2\theta \quad (34)$$

for ψ . This leaves the ambiguities of $\pm\psi$ in the definition of \mathbf{s} . The condition for diffraction requires a specification of whether the reflection was measured on the top ($s_1 > 0$) or bottom ($s_1 < 0$) of the recording film. Using this condition and the equation for $\cos \psi$ obtained from (34),

$$\cos \psi = \frac{1}{\cos \mu} (\sin^2 \mu + \cos 2\theta(1 + \sin^2 \mu)^{\frac{1}{2}}), \quad (35)$$

we have explicitly defined \mathbf{s} and \mathbf{s}_0 in terms of μ and θ .

R for the Weissenberg method is simply the $R_2(\varphi)$ of the previous section. The value of φ to be used is determined by

$$R_2(\varphi)\mathbf{x} = \mathbf{s} - \mathbf{s}_0 = \mathbf{d},$$

which is equivalent to the equation

$$\begin{pmatrix} x_1 & x_2 \\ x_2 & -x_1 \end{pmatrix} \begin{pmatrix} \cos \varphi \\ \sin \varphi \end{pmatrix} = \begin{pmatrix} d_1 \\ d_2 \end{pmatrix}. \quad (36)$$

Substitution of these results into (24) will then give, through (25) the required values of \mathbf{n}_i .

Buerger precession

Choose the crystal cartesian coordinate system such that \mathbf{e}_2 is along the precession axis, and \mathbf{e}_1 is along the goniometer head axis. In the notation of the precession camera,

$$\begin{aligned} \mathbf{s}_1 \cdot \mathbf{e}_2 &= s_1 \cos \nu, \\ \mathbf{s}_0 \cdot \mathbf{e}_2 &= s_0 \cos \mu. \end{aligned} \quad (37)$$

Define φ_0 and φ_1 as the angles between \mathbf{e}_1 and the projections of \mathbf{s}_0 and \mathbf{s} onto the $\mathbf{e}_1, \mathbf{e}_2$ plane. We can now write

$$\mathbf{s}_0 = \frac{1}{\lambda} \frac{1}{(1 + \cos^2 \mu)^{\frac{1}{2}}} \begin{pmatrix} \cos \varphi_0 \\ \cos \mu \\ \sin \varphi_0 \end{pmatrix}$$

and

$$\mathbf{s}_1 = \frac{1}{\lambda} \frac{1}{(1 + \cos^2 \nu)^{\frac{1}{2}}} \begin{pmatrix} \cos \varphi_1 \\ \cos \nu \\ \sin \varphi_1 \end{pmatrix}. \quad (38)$$

The precession geometry can best be treated by departing from the previous treatment of the other diffraction techniques and by treating the reciprocal lattice as stationary. We must now solve (23) and (34) for φ_0 and φ_1 for given μ and ν in order to define the diffraction direction for a given reciprocal lattice point. With an ambiguity of \pm in the $\sin \varphi_1$, we can solve (34) for $\cos \varphi_1$ and $\sin \varphi_1$ to give

$$\begin{pmatrix} \cos \varphi_1 \\ \sin \varphi_1 \end{pmatrix} = \begin{pmatrix} \cos \varphi_0 & \sin \varphi_0 \\ \sin \varphi_0 & -\cos \varphi_0 \end{pmatrix} \begin{pmatrix} g \\ \pm(1-g^2)^{\frac{1}{2}} \end{pmatrix}, \quad (39)$$

where

$$\left. \begin{aligned} g &= a_1 a_2 \cos 2\theta - \cos \mu \cos \nu \\ a_1 &= (1 + \cos^2 \mu)^{\frac{1}{2}} \\ a_2 &= (1 + \cos^2 \nu)^{\frac{1}{2}} \end{aligned} \right\}, \quad (40)$$

Substitution of (39) into (23) gives

$$\begin{pmatrix} \left(\frac{g-1}{a_1} - \frac{1}{a_0}\right) \left(\frac{\pm(1-g^2)^{\frac{1}{2}}}{a_1}\right) \\ \left(\frac{\mp(1-g^2)^{\frac{1}{2}}}{a_1}\right) \left(\frac{g-1}{a_1} - \frac{1}{a_0}\right) \end{pmatrix} \begin{pmatrix} \cos \varphi_0 \\ \sin \varphi_0 \end{pmatrix} = \lambda \begin{pmatrix} x_1 \\ x_3 \end{pmatrix}, \quad (41)$$

which can be solved to give

$$\begin{pmatrix} \cos \varphi_0 \\ \sin \varphi_0 \end{pmatrix} = \frac{\lambda}{\frac{1}{a_0^2} + \frac{1}{a_1^2} - \frac{2g}{a_1 a_0}} \begin{pmatrix} \left(\frac{g-1}{a_1} - \frac{1}{a_0}\right) \left(\frac{\mp(1-g^2)^{\frac{1}{2}}}{a_1}\right) \\ \left(\frac{\pm(1-g^2)^{\frac{1}{2}}}{a_1}\right) \left(\frac{g-1}{a_1} - \frac{1}{a_0}\right) \end{pmatrix} \begin{pmatrix} x_1 \\ x_3 \end{pmatrix}. \quad (42)$$

Substitution of (42) into (38) now gives \mathbf{s} and \mathbf{s}_0 which, in this case, immediately produce the \mathbf{n}_i through (24) since R^{-1} is the identity operation. Because reflection to a given point on the film occurs twice, corresponding to the \pm ambiguity in equation (42), both diffraction conditions must be considered in an absorption correction.

I would like to express to Prof. B. C. Carlson my

appreciation for his several, valuable discussions concerning coordinate systems.

References

- BOND, W. L. (1959). *Acta Cryst.* **12**, 375.
 BOOTH, A. D. (1955). *Numerical Methods*. London: Butterworths Scientific Publications.
 DEHANN, D. B. (1939). *Nouvelles Tables d'Integrals Definies*. New York: Stechert.

Acta Cryst. (1961). **14**, 526

A Theoretical Study of Pendellösung Fringes. Part I. General Considerations

By N. KATO

Division of Engineering and Applied Physics, Harvard University, Cambridge, Massachusetts, U.S.A.

(Received 19 May 1960)

The assumption of an incident plane wave is shown to be not adequate for single-crystal experiments of X-ray diffraction (Laue case). A dynamical theory of diffraction is formulated for a general type of monochromatic incident wave. Fundamental aspects of wave behavior are discussed in terms of wave-bundle considerations. Diffraction phenomena are classified by $\Delta\theta$ (an angular width of single-crystal reflection) and Ω_0 (a width in which the angular spectrum of an incident coherent wave takes an appreciable value). If $\Delta\theta \gg \Omega_0$, a plane-wave assumption is adequate. This is usually the case for electron diffraction. If $\Delta\theta \leq \Omega_0$, a spherical wave assumption is more appropriate and most of X-ray cases fall under this alternative. Furthermore, a criterion is given to distinguish between Fresnel and Fraunhofer diffraction in a crystalline medium. 'Pendellösung' fringes of X-rays (Kato & Lang, 1959) can be interpreted as Fraunhofer diffraction, while those of electrons are observed in a Fresnel diffraction region. The essential features of section patterns, particularly 'hook-shaped' fringes, can now be explained.

1. Introduction

In previous papers the first observations of X-ray Pendellösung fringes were reported (Lang, 1959; Kato & Lang, 1959). In addition, new types of diffraction fringes were obtained in section topographs under the experimental conditions fully described. These fringes are essentially due to interference between two kinds of crystal waves which correspond to different branches of the dispersion surface. Thus they have to be explained by a dynamical theory of diffraction.

'Pendellösung' interference effects were discovered first in electron-microscope experiments and could be well explained by dynamical theory.* Thus it seemed quite natural to apply this theory to X-rays because it is generally accepted that the theory is essentially the same for both electron and X-ray diffraction. However, as shown briefly in the previous paper (Kato & Lang, 1959), section patterns cannot be interpreted in a straightforward manner by the usual dynamical theory. In fact, they imply that we have to consider a divergent coherent wave instead of an

ideal plane wave as the incident wave (Kato, 1960b). The same is true for the general X-ray case, as shown in Section 2 by a simple argument. Hence, we must formulate the dynamical theory for a general type of incident monochromatic wave (Section 3). This is the main object of the present paper. In the following sections, only fundamental aspects of wave behavior are discussed on the basis of wave bundle considerations. A further development of the theory and detailed discussion of 'Pendellösung' phenomena will be reserved for the next paper.

2. Preliminary considerations

The usual dynamical theory may be summarized as follows. First, we assume a plane wave as an incident wave (PW assumption). As crystal waves we consider a sort of Bloch wave function. This is a general type of wave in a medium of periodically distributed scatterers. The incident wave and the crystal waves are connected by boundary conditions including the tangential continuity of wave vectors at the surfaces of the crystal (TC assumption). In the surrounding vacuum, we

* A detailed historical survey is given in the previous paper (Kato & Lang, 1959).